The Journal of Neuroscience, August 15, 1998, *18*(16):6059–6070

Synaptic Vesicular Localization and Exocytosis of L-Aspartate in Excitatory Nerve Terminals: A Quantitative Immunogold Analysis in Rat Hippocampus

Vidar Gundersen,[1] Farrukh A. Chaudhry,[1] Jan G. Bjaalie,[1] Frode Fonnum,[2] Ole Petter Ottersen,[1] and Jon Storm-Mathisen[1]

[1]*Department of Anatomy, Institute of Basic Medical Sciences, University of Oslo, Blindern, N-0317 Oslo, Norway, and* [2]*Vista, Norwegian Research Establishment, Division for Environmental Toxicology, N-2007 Kjeller, Norway*

To elucidate the role of aspartate as a signal molecule in the brain, its localization and those of related amino acids were examined by light and electron microscopic quantitative immunocytochemistry using antibodies specifically recognizing the aldehyde-fixed amino acids. Rat hippocampal slices were incubated at physiological and depolarizing [K^+] before glutaraldehyde fixation. At normal [K^+], aspartate-like and glutamate-like immunoreactivities were colocalized in nerve terminals forming asymmetrical synapses on spines in stratum radiatum of CA1 and the inner molecular layer of fascia dentata (i.e., excitatory afferents from CA3 and hilus, respectively). During K^+ depolarization there was a loss of aspartate and glutamate from these terminals. Simultaneously the immunoreactivities strongly increased in glial cells. These changes were Ca^{2+}-dependent and tetanus toxin-sensitive and did not comprise taurine-like immunoreactivity. Adding glutamine at CSF concentration prevented the loss of aspartate and glutamate and revealed an enhancement of aspartate in the terminals at moderate depolarization.

In hippocampi from animals perfused with glutaraldehyde during insulin-induced hypoglycemia (to combine a strong aspartate signal with good ultrastructure) aspartate was colocalized with glutamate in excitatory terminals in stratum radiatum of CA1. The synaptic vesicle-to-cytoplasmic matrix ratios of immunogold particle density were similar for aspartate and glutamate, significantly higher than those observed for glutamine or taurine. Similar results were obtained in normoglycemic animals, although the nerve terminal contents of aspartate were lower. The results indicate that aspartate can be concentrated in synaptic vesicles and subject to sustained exocytotic release from the same nerve endings that contain and release glutamate.

Key words: immunogold localization; L-aspartate; L-glutamate; electron microscopy; synaptic vesicles; nerve endings; astroglia; glutamine; hypoglycemia

Important requirements for classifying a substance as a neurotransmitter are that it should be localized in nerve terminals and released by regulated exocytosis. L-Glutamate (Glu) fulfills these criteria and is established as a transmitter at excitatory synapses in the mammalian brain (Fonnum, 1984; Ottersen and Storm-Mathisen, 1984a; headley and Grillner; 1990). However, the role of L-aspartate (Asp) in synaptic transmission is controversial. First, some electron microscopical immunogold studies of perfusion-fixed material have not detected Asp in nerve endings (Maxwell et al., 1990; Zhang et al., 1990; Montero, 1994), whereas positive results were reported in other experimental models (Merighi et al., 1991; Tracey et al., 1991; van den Pol, 1991; C. M. Hackney and K. K. Osen, unpublished results). Second, no study has yet shown uptake or content of Asp in isolated synaptic vesicles (Naito and Ueda, 1983; Maycox et al., 1988; Burger et al., 1991; Fykse et al., 1992). Third, in several studies, isolated cortical nerve terminals apparently failed to release Asp Ca^{2+}-dependently (Nicholls, 1989, 1993). However, Zhou et al. (1995) found that synaptosomes from hippocampus CA1 did release Asp in a Ca^{2+}-dependent manner. Likewise, a Ca^{2+}-dependent release of Asp has been reported from excitatory pathways *in vivo* (Girault et al., 1986; Paulsen and Fonnum, 1989) and from brain slices (Nadler et al., 1976, 1990; Toggenburger et al., 1983; Fonnum et al., 1986; Kangrga and Randic, 1990; Roisin et al., 1991; Klancnick et al., 1992). Asp was recently found to be released by exocytosis along with Glu from neuroendocrine pinealocyte microvesicles (Yatsushiro et al., 1997). In cultured cerebellar granule cells exogenous D-Asp entered synaptic vesicles and its release was exocytotic (Cousin et al., 1997; Cousin and Nicholls, 1997). Moreover, using synaptosomes McMahon et al. (1992) demonstrated that the K^+-induced release of Asp could be inhibited by tetanus toxin (TeTx). TeTx has been shown to inhibit neurotransmitter release by cleavage of synaptobrevin (Link et al., 1992; Schiavo et al., 1992), which is essential for the fusion of synaptic vesicles with the plasma membrane (Link et al., 1994).

Our previous light microscopic immunocytochemical results with hippocampal slices (Gundersen et al., 1991) indicated that Asp, similar to Glu, was localized in nerve ending-like dots in the terminal fields of excitatory afferents in hippocampus. On K^+-depolarization, Glu and Asp were depleted from these dots and appeared in glial cells in a Ca^{2+}-dependent manner.

Received Feb. 24, 1998; revised May 18, 1998; accepted May 26, 1998.

This work was supported by the Norwegian Research Council and by funds managed by the Faculty of Medicine, University of Oslo and the Norwegian Academy of Science and Letters. This research was part of EU Biomed2 Concerted Action Grant BMH1-CT94–1248. We thank Anne Skotte, Anna Torbjørg Bore, Kari Ruud, Carina Knutsen, and Gunnar Lothe for technical assistance. We are grateful to Statens Seruminstitut, Copenhagen, Denmark, for the gift of tetanus toxin.

Correspondence should be addressed to Vidar Gundersen, Anatomical Institute, University of Oslo, P.O. Box 1105 Blindern, 0317 Oslo, Norway.

Here we extend our investigations using quantitative immunogold electron microscopy in hippocampal slices and intact brain. In addition we exploit the hypoglycemic model, in which brain Asp levels are strongly increased *in vivo* (Engelsen and Fonnum, 1983) and the morphological preservation is good, to investigate the intraterminal distribution of Asp. We address the following questions: (1) Is Asp localized in excitatory nerve terminals, and, if so, is it colocalized with Glu? (2) Is Asp concentrated in synaptic vesicles in the terminals? (3) Can inhibition of exocytosis block the K^+-induced depletion of Asp from nerve endings? (4) Is glutamine (Gln) a precursor of nerve terminal Asp?

MATERIALS AND METHODS

Preparation and incubation of hippocampal slices. This was done largely as before (Gundersen et al., 1991, 1993). Rats derived from the Wistar strain were anesthetized with halothane, decapitated, and the brains were put in ice-cold normal Krebs' solution (in mM: 130 NaCl, 3 or 5 KCl, 15 sodium phosphate buffer, pH 7.4, 1.2 $CaCl_2$, 1.2 $MgSO_4$, and 10 glucose). Hippocampi were sliced (300 μm) and incubated at 30°C (in some experiments after preincubations at 30°C) in oxygenated normal (3 or 5 mM K^+) or depolarizing (55 mM K^+; Na^+ reduced to 80 mM) Krebs' solutions (10 ml/six to eight slices) in the presence and absence of different additives. The slices were kept on a nylon mesh in a glass beaker with a continuous flow of O_2 over the surface of the medium. During the incubations, the solutions were replaced every 10 min with oxygenated fresh media.

In experiments with low Ca^{2+}, the Ca^{2+} concentration was reduced to 0.1 mM and the Mg^{2+} concentration increased to 10 or 1.0 mM EGTA added to the incubation medium.

In a series of experiments, the slices were preincubated in normal Krebs' solution for 2 hr in the presence and absence of TeTx (from Statens Seruminstitut, Copenhagen, Denmark; 0.25 mg/ml). Thereafter, fresh, oxygenated physiological or depolarizing Krebs' solutions without TeTx replaced the preincubation media, and the slices were incubated for another hour. (Pilot experiments analyzed light-microscopically indicated that 0.03 mg/ml was effective, but 0.25 mg/ml was selected to get a robust and reproducible response). In additional experiments, purified TeTx from another supplier (Almone Laboratories, 0.03 mg/ml) was used with similar results.

After incubation, the slices were fixed for 1 hr at room temperature (~22°C) in a mixture of 2.5% glutaraldehyde and 1% formaldehyde (freshly prepared from paraformaldehyde) in sodium phosphate buffer (0.1 mM, pH 7.4). The slices were stored at 4°C in the same fixative with 0.1% sodium azide added.

Hypoglycemic and normoglycemic perfusion-fixed tissue. Five fasted Wistar rats were made hypoglycemic by intraperitoneal injection of insulin, as described before (Engelsen and Fonnum, 1983). When the rats went into a coma, they were given an injection of pentobarbital (100 mg/kg, i.p.) and fixed by perfusion through the heart with glutaraldehyde and formaldehyde (see above) (Ji et al., 1991). Blood samples for glucose analysis were taken immediately before the fixation. The blood glucose concentrations were between 1.0 and 1.5 mM.

Five normoglycemic rats were similarly anesthetized and perfusion-fixed.

Pre-embedding light microscopic immunocytochemistry. TeTx is a relatively large protein (150 kDa), which means that it penetrates poorly into the tissue. Thus, in the TeTx experiment the slices were subjected to the immunocytochemical procedure without resectioning to stain only the surface of the slices. In the other experiments the slices were soaked in 30% sucrose before resectioning at 20 μm on a freezing microtome. The sections and slices were processed free-floating in plastic wells with the Asp (no. 435; dilution 1:1500) and Glu (no. 607; dilution 1:5000) antisera with additions (Fig. 1) in the presence of 0.5% Triton X-100 according to a three-layer biotinylated antibody-streptavidin-biotinylated peroxidase method (Hsu et al., 1981).

Postembedding electron microscopic immunocytochemistry. Slices from each experimental condition described above and specimens from perfusion-fixed hypoglycemic animals were treated with 2% uranyl acetate in 0.15 M sodium acetate buffer, pH 6.0, on ice. This was used instead of osmium tetroxide, which inhibits the labeling of Asp (Zhang et al., 1993) and D-Asp (Gundersen et al., 1993, 1995). The specimens were then dehydrated in ethanol and embedded in Durcupan (ACM).

Ultrathin sections (gold) were cut (at right angles to the slices so that the observations could be made at defined distance from the slice surface), mounted on nickel grids, and processed according to a two-layer immunogold procedure (Somogyi et al., 1986; Ottersen, 1987, 1989a). The first antibody (raised in rabbit, see below) recognized fixed amino acid, and the secondary antibody (recognizing rabbit Ig) was coupled to colloidal gold particles.

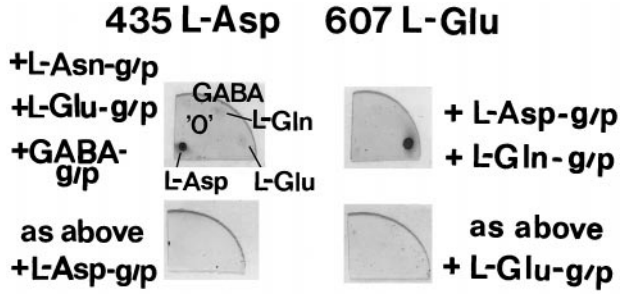

Figure 1. Test filters (processed together with the tissue sections presented in Fig. 5) illustrating the immunocytochemical specificity. The spots (0.1 μl) contained brain macromolecules conjugated by a glutaraldehyde/formaldehyde (g/p) mixture to amino acids L-Asp, L-Glu, L-Gln, and GABA, or only treated with glutaraldehyde/formaldehyde ("0"). The diluted 435 L-Asp and 607 L-Glu antisera were mixed with soluble g/p complexes of amino acids [L-asparagine (L-Asn), L-Glu, GABA, L-Asp, and L-Gln; 0.2 mM each] as indicated before the sera were used on the test and tissue sections. Note that the L-Asp antiserum selectively stained the L-Asp spot, whereas the L-Glu antiserum selectively stained the L-Glu spot. The staining of test filters and tissue sections was abolished by preabsorption with g/p complexes (0.3 mM) of the amino acid used for immunization.

In the slice experiments in which exocytosis was blocked, the sections were first treated with the 435 Asp antiserum (dilution 1:300) and then with the 607 Glu antiserum (dilution 1:3000) to visualize Asp and Glu in the same terminals. Between the first and the second step the sections were treated with formaldehyde vapor at 80°C for 1 hr to prevent interference between the sequential incubations (Wang and Larsson, 1985; Ottersen et al., 1992). A secondary antibody coupled to gold particles with a diameter of 15 nm was used in the first step, and a secondary antibody with 30 nm gold particles was used in the second step. Because the aldehyde vapor treatment may reduce the labeling intensity by denaturing tissue epitopes, single labeling (15 nm particles) of neighboring ultrathin sections was used as an alternative procedure. The two procedures gave similar results. Additional sections from the TeTx experiments were single-labeled with the taurine (Tau) antiserum (no. 286, dilution 1:2000).

The perfusion-fixed tissue from hypoglycemic rats was cut in series and neighboring ultrathin sections were single-labeled with the 435 Asp and the 607 Glu antisera using the same dilutions as above. Some sections were also labeled with the 286 Tau antiserum and the Gln antiserum (no. 34, dilution 1:300).

Specimens from perfusion-fixed normoglycemic animals were cryoprotected in glycerol, quickly frozen in liquid propane, freeze-substituted with methanol, embedded in Lowicryl HM 20, and further processed for single labeling as described by Chaudhry et al. (1995). Triton X-100 was added to the primary antibodies (Phend et al., 1992). As a high sensitivity was obtained, the antibodies were used at the following dilutions: 435 Asp 1:3000, 607 Glu 1:10000, and 34 Gln 1:12000.

Sera and specificity controls. The antisera were raised in rabbits essentially as first described (Storm-Mathisen et al., 1983) by immunizations with glutaraldehyde–formaldehyde bovine serum albumin conjugates of the respective amino acids. The Asp, Glu, Tau, and Gln antisera have been characterized previously and proven highly specific when used as described (no. 435, Zhang et al., 1993; no. 286, Amiry-Moghaddam et al., 1994; no. 607, Ericson et al., 1995 and Broman et al., 1993; no. 34, Laake et al., 1986). The L-Asp antiserum showed slight cross-reactivities against Glu, L-asparagine, and D-Asp in pilot immunogold experiments. Soluble glutaraldehyde–formaldehyde (weight proportion 2.5:1) complexes of Glu, L-asparagine, and GABA (0.2 mM each amino acid) were therefore added to the diluted antibody preparation 3–24 hr before applying it to the sections. D-Asp complexes were omitted because of the very low concentration of D-Asp in the adult brain (Dunlop et al., 1986; Hashi-

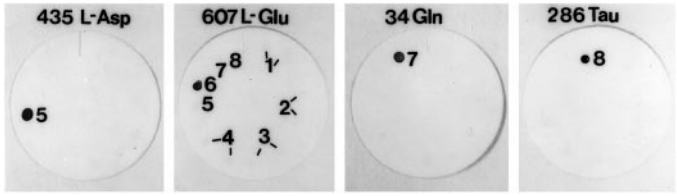

Figure 2. Test filters showing that the antisera do not react with synaptic vesicle proteins or other tissue macromolecules. The test spots (0.1 μl, 0.1 μg protein) contained macromolecules from synaptic vesicles, cytosol, and mitochondria, as well as amino acids conjugated to tissue macromolecules as in Figure 1. The filters with the spots were fixed with glutaraldehyde/formaldehyde, washed, and then exposed to the L-Asp, Glu, Gln, or Tau antibodies (final dilutions 1:300, 1:3000, 1:100, 1:3000, respectively). Note that for each antibody only the spot with the corresponding amino acid conjugate was labeled. The numbers indicate: 1, synaptic vesicles; 2, cytosol from synaptosomes; 3, nonsynaptosomal cytosol; 4, mitochondria from synaptosomes; 5, conjugated L-Asp; 6, conjugated Glu; 7, conjugated Gln; and 8, conjugated Tau.

moto et al., 1993), as confirmed by the lack of labeling of hippocampal slices with a D-Asp antiserum (Gundersen et al., 1993). In addition, for this study aldehyde and protein reactivities were absorbed from the Asp antiserum on an agarose column bearing glutaraldehyde–formaldehyde-treated bovine serum albumin and IgG subsequently isolated on a protein A column (dilutions given are with respect to the crude serum). The Glu antiserum was used with the addition of 0.2 mM glutaraldehyde–formaldehyde-treated Asp and Gln.

As an intrinsic specificity control for each incubation of the preembedding type, conjugates of different amino acids linked to brain macromolecules by glutaraldehyde–formaldehyde were spotted on cellulose nitrate–acetate filters (0.45 μm pores) and processed together with the tissue sections (Ottersen and Storm-Mathisen, 1984b) (Fig. 1). For postembedding immunocytochemistry, such conjugates were freeze-dried and embedded in Durcupan ACM (Ottersen, 1987). Ultrathin sections were cut, mounted on nickel grids, and incubated together with the tissue sections. The concentration of the fixed amino acids in the embedded conjugate clumps is ~100 mM (Ottersen, 1989b). These test systems showed that the immunolabeling obtained in the present study was highly specific. Furthermore, the Asp, Glu, Tau, and Gln immunoreactivities of tissue and test sections were blocked by adding 0.3 mM aldehyde-treated Asp, Glu, Tau, or Gln to the respective antisera. The test systems also showed that there was no interference between the first and second step in the double-labeling experiments.

To check for possibly selective cross-reactivity of the antibodies with synaptic vesicle components, rat brain tissue was fractionated according to Whittaker et al. (1964) with modifications as described by Fykse and Fonnum (1988). Fractions of lysed synaptosomes, synaptic vesicles, mitochondria, and cytosol, as well as the nonsynaptosomal cytosolic supernatant from whole brain were tested. Protein concentrations were determined, and the fractions were concentrated (vesicles, by lyophilization) or diluted (synaptosomal cytosol, with H_2O) to 2 μg/μl. The fractions were spotted on cellulose ester filters along with the amino acid conjugates at the same final protein concentrations (2 μg/μl). After drying, the filters were rinsed in sodium phosphate buffer (0.1 M, pH 7.4) for 30 min to remove free amino acids, fixed over-night in the same aldehyde mixture as used for tissue fixation, rinsed again in sodium phosphate buffer, and processed with the antibodies in the same way as frozen sections. The antibody concentrations were at least as high as those used for postembedding immunocytochemistry. There was only labeling of the corresponding amino acid conjugate (Fig. 2), i.e., no indication of cross-reactivity between the antisera and vesicular proteins.

Light microscopic determination of the density of immunoreactive glial cells. The numbers of Asp and Glu positive glial profiles in stratum radiatum of CA1 and in stratum moleculare of fascia dentata were counted in the light microscope with a 40× objective within an area of 0.05 mm^2. The densities of immunoreactive glial cells were calculated and the data were statistically evaluated by a two-sample Student's *t* test (two-tails).

Quantitative immunogold analysis. The ultrathin sections were viewed in a Philips CM 10 electron microscope. Electron micrographs were taken randomly in the st. radiatum of CA1 and in the inner third of st. moleculare of fascia dentata at 6300× primary magnification. The quantifications were done at 48,000× final magnification.

In the slice experiments with TeTx, micrographs were taken within 30 μm of the surface of the slices. (Here the texture of the slices was loose, which should permit penetration of the 150 kDa toxin). In the other slice experiments, micrographs were taken along random trajectories across the thickness of the slice. Asp-like immunoreactivity (Asp-LI), Glu-like immunoreactivity (Glu-LI), and (in the TeTx experiments) Tau-like immunoreactivity (Tau-LI) were quantified in terminals making asymmetrical synapses in their postsynaptic spines, as well as in dendritic shafts, pyramidal cells, and glial cells (identified by the presence of filaments and/or by contact with capillaries).

In the perfusion-fixed hypoglycemic tissue, the Asp, Glu, Gln, and Tau immunoreactivities were quantified over synaptic vesicle clusters and over cytoplasmic matrix in terminals forming asymmetrical junctions on spines. Vesicular localization of different amino acids was not investigated in the same terminal because synaptic vesicle clusters evident in one section often became blurred in the next one. However, to study colocalization, Asp-LI and Glu-LI were quantified in the same terminals synapsing asymmetrically on spines in stratum radiatum of CA1 in neighboring ultrathin sections.

In the freeze-substituted normoglycemic material, in which synaptic vesicles were more clearly distinguished, gold particles were quantified over individual vesicular profiles as opposed to nonvesicular, nonmitochondrial areas (cytoplasmic matrix). A gold particle was assigned to a vesicle if its center was inside the outer border of the vesicular contour. (Because of the size of the gold particles and the antibody molecules, some intravesicular antigenic sites will result in extravesicular particles and vice versa. On the other hand, some particles whose centers overlie vesicular contours may be attributable to antigenic sites in the cytoplasmic matrix over or underneath the vesicle.)

The areas of the various cellular and subcellular elements, over which numbers of gold particles were recorded, were determined by point-counting using an overlay screen (Gundersen et al., 1988), and the gold particle densities were calculated. The results were statistically evaluated (Statistica), first by a nonparametric ANOVA test (Kruskal–Wallis) before performing a nonparametric test (Mann–Whitney *U* test, two tails) to investigate differences in mean gold particle densities between individual experimental groups. When statistical differences were obtained with the Mann–Whitney test, the ANOVA test always showed significant overall variation among the groups ($p < 0.05$).

The relationship between the Asp and Glu immunogold particle densities and the concentrations of fixed Asp and Glu in the tissue was nearly linear, as assessed by simultaneously processed ultrathin sections containing a dilution series of amino acids conjugated to brain protein (Ottersen, 1989b).

The spatial association of Asp and Gln immunogold particles with vesicles was further studied in freeze-substituted normoglycemic material. With the use of a program, Micro Trace (Leergaard and Bjaalie, 1995), the localization of the centers of synaptic vesicles and gold particles was digitized and saved on file. Custom software was used to calculate the intercenter distance from each gold particle to its nearest neighboring vesicular profile. Altogether 139 and 271 intercenter distances from immunogold particle to nearest neighboring vesicle profile were measured in 11 L-Asp labeled and 11 Gln-labeled terminals, respectively. The distances were sorted into bins of 20 nm. The frequencies of intercenter distances for each bin were calculated, and the data were statistically evaluated by a Yates' corrected χ^2 test (Statistica).

Materials. Tetanus toxin prepared according to the World Health Organization Manual BLGUNDP 77.2 Rev.1 was a gift from Statens Seruminstitut. Tetanus toxin was also obtained from Almone Labs, Jerusalem, Israel. Durcupan ACM was purchased from Fluka (Buchs, Switzerland), and Lowicryl HM20 was purchased from Electron Microscopy Sciences (Fort Washington, PA). Amino-oxoacetic acid (AOAA) and EGTA were from Sigma (St.Louis, MO) and glutaraldehyde (25%, EM) from TAAB (Reading, UK). Cellulose ester filters were from Millipore (Bedford, MA). Anti-rabbit Ig (biotinylated Ig from goat), streptavidin-biotinylated horseradish peroxidase complex, and Auroprobe GAR 15 and GAR 30 were obtained from Amersham (UK). These immunoreagents were diluted as recommended by the manufacturer.

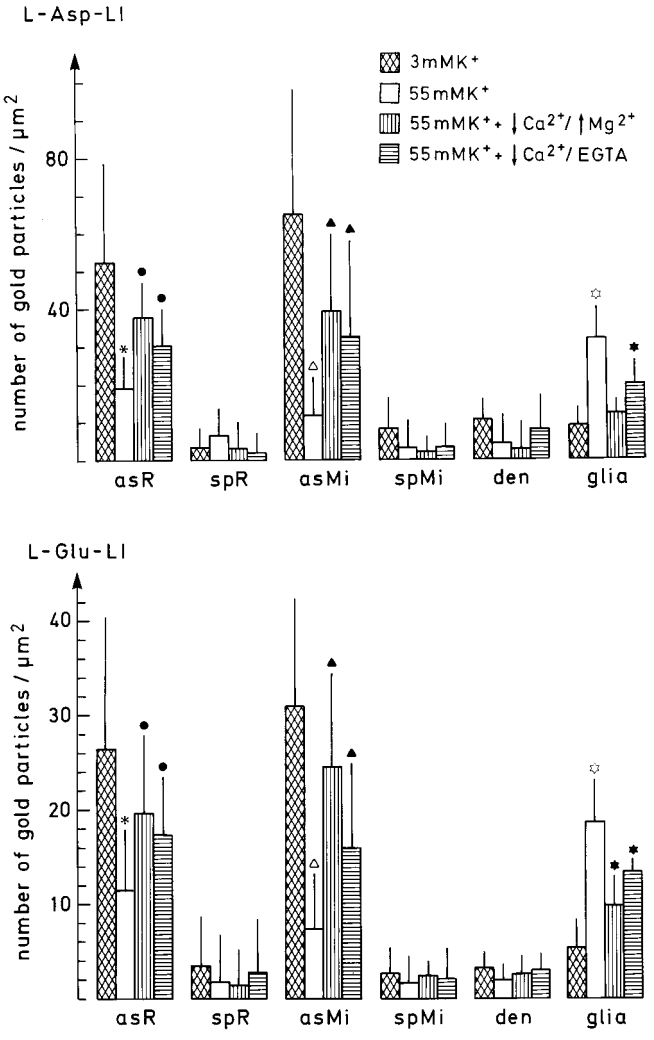

Figure 3. Double-labeling quantitation of L-Asp-LI and L-Glu-LI in different tissue compartments in slices incubated for 1 hr under control (3 mM K^+) and depolarizing conditions (55 mM K^+) at physiological (1.3 mM) or low Ca^{2+} concentrations. The low Ca^{2+} medium contained 0.1 mM Ca^{2+} and 10 mM Mg^{2+} or 1.0 mM EGTA. The values are mean numbers of gold particles per square micrometer ± SD in *n* tissue element profiles corrected for background labeling over empty resin (average 1.1 and 1.6 particles per square micrometer for L-Asp and L-Glu, respectively). The data shown here are from one animal; similar results were obtained in another animal in a separate experiment. Each profile was labeled with both the L-Asp and the L-Glu antiserum, respectively, on the same ultrathin section. The particle densities are arbitrary units (simultaneously processed test sections with known concentrations of Asp and Glu indicated a lower labeling efficiency for Glu, showing that the glutamate- and aspartate-labeling densities in excitatory nerve terminals at control conditions correspond to a concentration of ~4 mM in the fixed tissue). At control conditions, the media with the low Ca^{2+}-concentration did not alter the level of L-Asp or L-Glu immunoreactivity in any of the profiles (data not shown). Symbols used here and in Figure 6: *asR*, terminals forming asymmetrical synapses with spines in stratum radiatum of CA1 (*spR*) (see Fig. 5 for illustration of strata); *asMi*, terminals forming asymmetrical synapses with spines in the inner third of the molecular layer of fascia dentata (*spMi*); *den*, dendritic shafts in stratum radiatum of CA1 and the inner third of the molecular layer of fascia dentata; *glia*, glial cells (in CA1 and fascia dentata) identified by fine filaments or contact with capillaries. *Asterisks* and *open triangles*, Values in asR and asMi at 55 mM K^+ ($n = 25$ and 20) were significantly different ($p < 0.02$) from the values at 55 mM K^+ with low Ca^{2+}–high Mg^{2+} ($n = 28$ and 21) and low Ca^{2+}–EGTA ($n = 30$ and 23) and from the values at 3 mM K^+ ($n = 27$ and 23). *Filled circles* and *filled triangles*, Values in asR and asMi at 55 mM K^+ when exocytosis was blocked were significantly different ($p < 0.05$) from the values at 3 mM K^+. *Open stars*, Values in glia at 55 mM K^+ ($n = 13$) were significantly different ($p < 0.01$) from the values at 55 mM K^+ with low Ca^{2+}–high Mg^{2+} ($n = 11$) and low Ca^{2+}–EGTA ($n = 12$) and from the values at 3 mM K^+ ($n = 10$). *Filled stars*, Values at 55 mM K^+ when exocytosis was blocked were significantly different ($p < 0.02$) from the values at control conditions. In *spR*, *spMi*, and *den* the numbers of profiles were between 12 and 30.

RESULTS

Depolarization-induced redistribution of immunoreactivities is Ca^{2+}-dependent

Light microscopy showed that K^+-induced depolarization causes depletion of Asp-LI and Glu-LI from nerve ending-like dots in the excitatory terminal areas of hippocampus and a simultaneous accumulation of the two immunoreactivities in glial cells (data not shown). The effect of high K^+ was strongly reduced by incubating the slices in a medium with low Ca^{2+} (0.1 mM) and high Mg^{2+} (10 mM) concentrations. Inhibiting Ca^{2+}-influx during depolarization without increasing the Mg^{2+} concentration (making the medium almost devoid of free Ca^{2+} ions by 1 mM EGTA) also maintained the nerve terminal-staining patterns of Asp-LI and Glu-LI. It reduced the number of Asp- and Glu-stained glial cells per area (by a factor of 2.6 and 3.7, respectively; $p < 0.02$ relative to high K^+ with normal Ca^{2+}). The latter effect was somewhat less than that of a medium containing a high Mg^{2+} concentration (areal density of Asp and Glu immunoreactive glial cells reduced by a factor of 5.9 and 7.5, respectively, $p < 0.01$ relative to high K^+ with normal Ca^{2+}).

At 3 mM K^+, quantitative immunoelectron microscopy revealed that gold particles signaling Asp and Glu (Fig. 3) were localized at high densities over nerve terminals making asymmetrical synapses on spines in stratum radiatum of CA1 and in the inner third of the molecular layer of fascia dentata (i.e., excitatory nerve terminals originating from the CA3 pyramidal cells and hilar mossy cells, respectively). Postsynaptic spines, dendritic shafts, pyramidal cell bodies, and glial cells were weakly labeled, confirming our previous light microscopical observations (Gundersen et al., 1991) that the Asp and Glu laminar distribution patterns were attributable to stained nerve endings. The labeling patterns produced by the Asp and Glu antisera in tissue incubated at 3 mM K^+ were not affected by the low Ca^{2+} conditions. (Note that here and in the other experiments the particle densities for the different amino acids cannot be directly compared because the labeling efficiencies are not the same).

At 55 mM K^+, Asp-LI and Glu-LI were depleted from the said excitatory types of terminal, whereas the densities increased in glial cells (Fig. 3). Depolarizing the tissue with 55 mM K^+ did not cause the synaptic vesicles to disappear (Fig. 4*A*, *inset*), suggesting that the vesicles have reduced amino acid contents. The effect of K^+ stimulation was confined to the presynaptic element of the asymmetrical synapses (Fig. 3).

Decreasing the Ca^{2+} concentration to 0.1 mM in the presence of either 10 mM Mg^{2+} or 1.0 mM EGTA significantly reduced the effect of depolarization on the levels of Asp-LI and Glu-LI in the terminals forming asymmetrical synapses (Fig. 3). The high K^+-induced appearance of Asp and Glu immunogold particles in glial cells was reduced or prevented by the low Ca^{2+} conditions (Fig. 3). Confirming the light microscopical observations, the medium containing a high concentration of Mg^{2+} ions was somewhat more efficient than EGTA medium in preventing depolarization-induced changes in the neuronal and glial labeling.

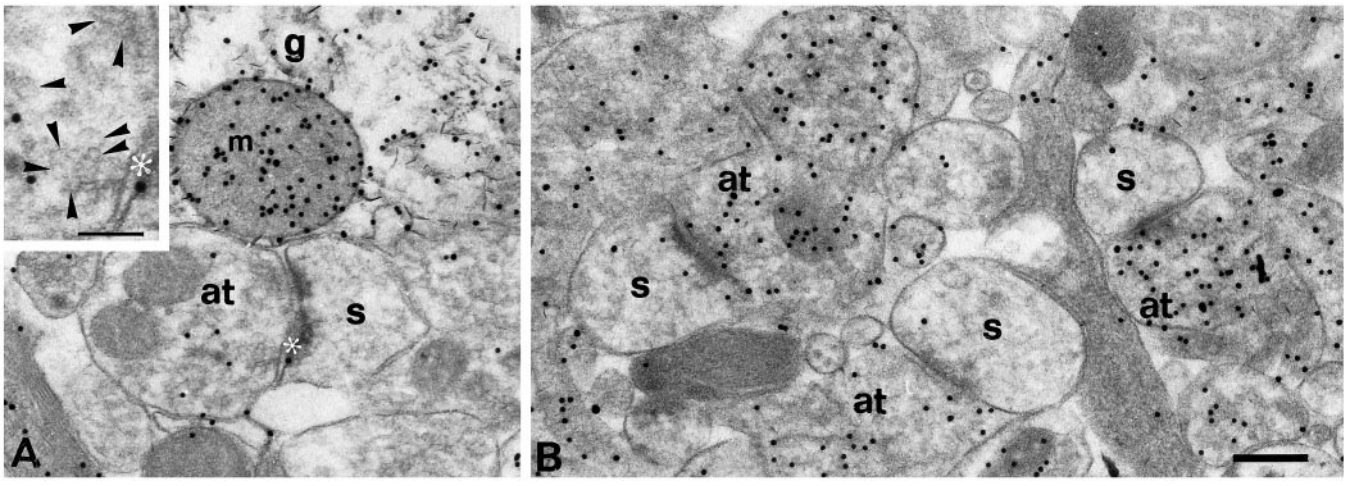

Figure 4. Electron micrographs showing gold particles signaling L-Asp in stratum radiatum CA1 of hippocampal slices incubated at 55 mM K^+ (*A*) and 55 mM K^+ with low Ca^{2+}–high Mg^{2+} (*B*) for 1 hr before fixation. In *A* note that the terminal with asymmetrical junction (*at*) on a spine (*s*) is weakly labeled, whereas the similar type of terminal in *B* is strongly labeled. The glial profile (*g*) in *A* is strongly immunopositive for L-Asp. [The glial mitochondrion (*m*) is heavily labeled, other mitochondria are not]. In *B* also note the contrast in labeling between the terminals (*at*) and the spines (*s*). *A*, *inset*, Higher power photomicrograph of a part of the terminal (*at*) in *A* showing individual synaptic vesicles with diameters of ~20–60 nm (*arrowheads*), which is in the same range as in this type of terminal *in vivo* (Harris and Sultan, 1995). *Asterisks*, Synaptic cleft. Scale bars: *A*, *B* 200 nm; *inset* 100 nm.

Effects of tetanus toxin

To interfere with the exocytotic process at the fusion step, slices were exposed to TeTx for 2 hr before depolarization (three experiments). These slices maintained the Asp and Glu laminar-staining patterns, and the densities of stained glial cells were considerably reduced compared with depolarized slices not pre-incubated with TeTx (Fig. 5). At depolarizing conditions TeTx reduced the numbers of Asp- and Glu-positive glia/mm^2 by a factor of 4.1 and 7.3, respectively, i.e., similar to the effects of low Ca^{2+}-conditions (see above).

Quantitations at the subcellular level also demonstrated that the effect of TeTx on the depolarization-induced changes in Asp-LI and Glu-LI (Fig. 6) was comparable to the effect of low Ca^{2+} (Fig. 3). At 55 mM K^+ with TeTx the levels of gold particles signaling Asp and Glu in terminals making asymmetrical synapses in stratum radiatum and in the inner third of the molecular layer of fascia dentata were significantly higher than at 55 mM K^+ without TeTx (Figs. 6, 7). However, they were lower than the values in control conditions. TeTx reduced the accumulation of immunoreactivity in glial cells at 55 mM K^+, but the values were not fully reversed to those seen at 3 mM K^+ plus TeTx (Fig. 6). The toxin did not significantly alter the levels of Asp-LI or Glu-LI in postsynaptic spines, dendritic shafts, and pyramidal cell bodies at 55 mM K^+, nor their levels at 3 mM K^+ in any of the profiles included in the study (Fig. 6).

In contrast to Asp-LI and Glu-LI, Tau-LI was not significantly reduced in terminals with asymmetrical synapses during depolarization, and TeTx did not influence the density og Tau immunogold particles in these terminals at control or depolarizing conditions (Fig. 6). Likewise, Tau-LI was unchanged in spines, dendritic shafts, and glial cells during all experimental conditions.

In a separate experiment (with TeTx from Almone Labs) the densities of Asp and Glu immunogold particles (mean number of gold particles/μm^2 ± SD; labeling efficiencies different from those in Fig. 6) in excitatory-type nerve terminals in st. radiatum of CA1 at depolarizing conditions with TeTx (67 ± 31 and 122 ± 48, n = 20 and 19) were the same as the densities at control conditions (65 ± 28 and 125 ± 51, n = 22 and 21), and again, significantly higher than the densities at depolarizing conditions without TeTx (27 ± 12 and 38 ± 16, n = 18) ($p < 0.01$, Mann–Whitney, two tails).

Effects of glutamine

In slices incubated with 0.5 mM Gln (the CSF concentration), the densities of Asp and Glu immunogold particles (mean number of gold particles/μm^2 ± SD) in N terminals making asymmetrical synapses in stratum radiatum of CA1 were 32.7 ± 15.5 (n = 51) and 70.5 ± 27.2 (n = 42), respectively, at 5 mM K^+. At 40 mM K^+, the corresponding values were 40.1 ± 16.7 (n = 46) and 75.9 ± 25.1 (n = 39), and at 55 mM K^+ the values were 27.7 ± 11.1 (n = 47) and 67.5 ± 27.2 (n = 38), respectively. Gln thus alleviated the depolarization-induced reduction in the densities of immunogold particles seen in the absence of Gln. Furthermore, in line with the previous qualitative light microscopic results (Gundersen et al., 1991), in the presence of Gln there was a significant increase in Asp-LI in excitatory nerve terminals at 40 mM K^+ compared with Asp-LI at 5 mM K^+ and at 55 mM K^+ ($p < 0.05$, Mann–Whitney, two tails).

Effects of amino-oxyacetic acid

To investigate whether the changes observed on depolarization could depend on interconversion of Asp and Glu via Asp-AT, AOAA was used at a concentration (3 mM) sufficient to totally block the conversion of Asp to Glu in synaptosomes (Kvamme, 1983). Addition of AOAA to the preincubation (20 min) and incubation (1 hr) media had no effect on the Asp- and Glu-staining patterns in the control or depolarized situations (light microscopical observations only).

Reversibility

When the slices were first incubated at 55 mM K^+ (1 hr) and then at 5 mM K^+ (30 min) the Asp- and Glu-staining patterns changed from a predominantly glial pattern to the pattern of fine punctate staining seen in slices exposed to 5 mM K^+ only. At the electron microscopic level the densities of Asp-LI and Glu-LI in terminals

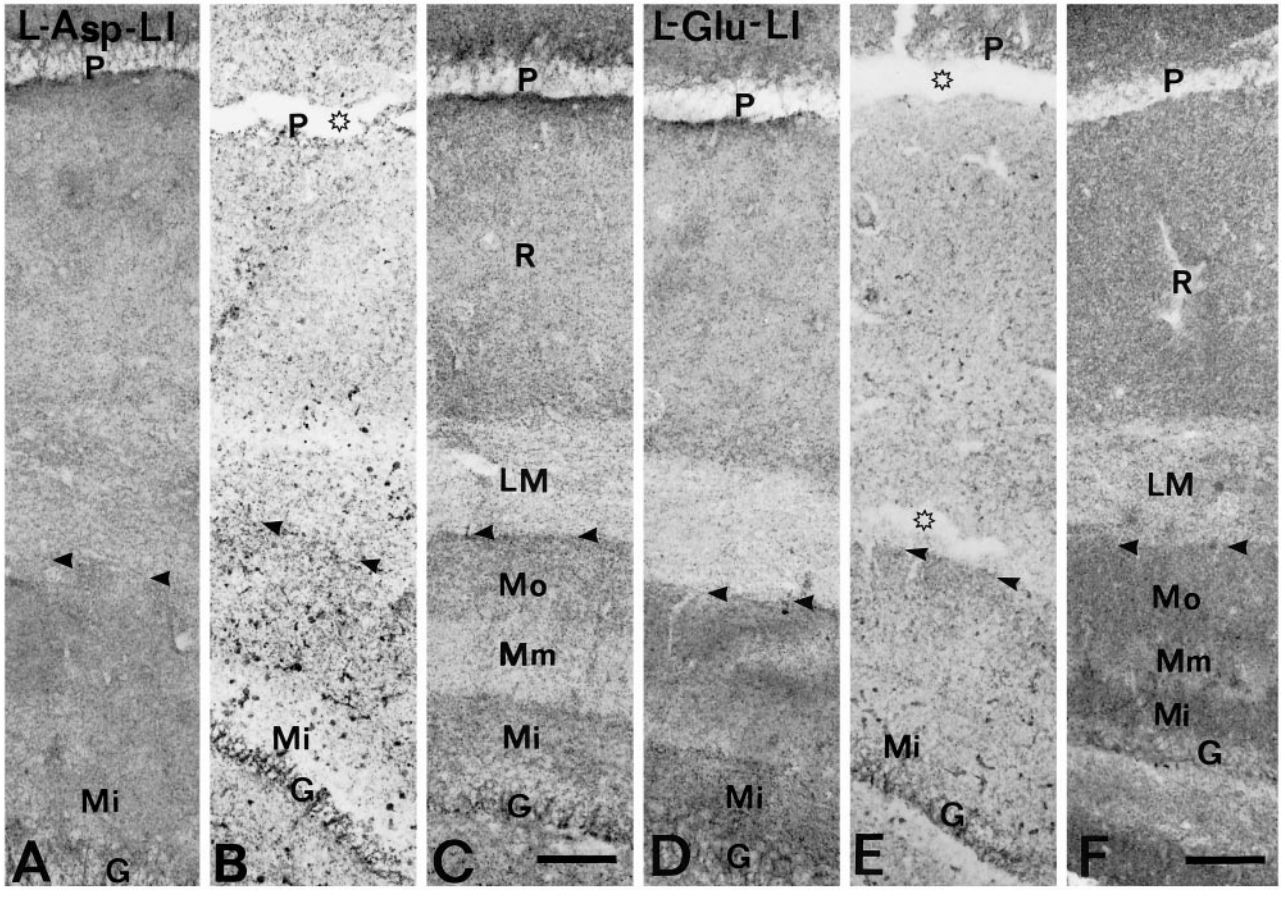

Figure 5. Light micrographs showing the effect of depolarization and TeTx on L-Asp-LI (*A–C*) and Glu-LI (*D–F*) in CA1 and fascia dentata of hippocampal slices. The slices were incubated as follows: *A*, *D*, 3 mM K^+ for 3 hr; *B*, *E*, 55 mM K^+ for 1 hr after preincubation for 2 hr at 3 mM K^+; and *C*, *F*, 55 mM K^+ (without TeTx) for 1 hr after preincubation for 2 hr at 3 mM K^+ in the presence of TeTx. To stain preferentially the tissue accessible to TeTx, the slices were immunoreacted with the antibodies without resectioning and the surface photographed. Note that TeTx prevented the change from a nerve terminal-like staining pattern (*fine dots*) to a predominantly glial pattern (*coarse processes*) at depolarizing conditions. *P*, *R*, *LM*, Layers of hippocampus (pyramidale, radiatum, and lacunosum moleculare, respectively). *Mo*, *Mm*, *Mi*, *G*, Layers of area dentata (outer, middle moleculare, inner moleculare, and granulare, respectively). *Arrowheads* mark the obliterated fissura hippocampi. *Open stars* mark tears in the slice. Scale bar, 100 μm.

with asymmetrical synapses were normalized after incubating the slices at 5 mM K^+ after 55 mM K^+ (compare Fig. 4). This indicates that the depolarization-induced depletion of Asp-LI and Glu-LI is not attributable to damage such as disruption of nerve terminal membranes and that the tissue is well enough preserved to recover and build up a new pool of Asp and Glu in the terminals.

Vesicular localization of aspartate in perfusion-fixed hypoglycemic tissue

The suboptimal morphological preservation of the slices, which is a combined consequence of the *in vitro* incubation and the omission of osmium tetroxide, did not allow a precise investigation of the spatial relation between Asp-LI and synaptic vesicles. Because the level of demonstrable Asp-LI in normal perfusion-fixed tissue embedded in epoxy resin is low (see below), studies of vesicular localization cannot be easily done using such tissue. One way of overcoming these obstacles is to induce hypoglycemia, a treatment that elevates brain levels of Asp (Engelsen and Fonnum, 1983), before fixing the brains by perfusion. In this way the immunolabeling may be performed on tissue with preserved morphology that, at the same time, has increased levels of Asp. In terminals forming asymmetrical synapses on spines in stratum radiatum of CA1 the Asp-LI and Glu-LI particle densities over synaptic vesicle clusters exceeded those over cytoplasmic matrix by factors of 2.0 and 2.4, respectively (Figs. 8, 9). In contrast, Gln-LI and Tau-LI were not enriched over synaptic vesicle clusters versus cytoplasmic matrix (Fig. 9).

Colocalization of aspartate and glutamate

In the perfusion-fixed hypoglycemic tissue Asp-LI and Glu-LI were colocalized at high densities in the terminals forming asymmetrical synapses compared with their postsynaptic spines (Fig. 10). There was a significant positive correlation between the density of gold particles signaling Asp and that of ones signaling Glu in these terminals (Fig. 11). Quantitative examination of double-labeled sections from the Ca^{2+} and TeTx experiments as well as visual investigation of neighboring sections from the TeTx experiments also showed that immunoreactivities for Asp and Glu were localized in the same terminals forming asymmetrical synapses on spines. This was true both under control conditions and under conditions in which transmitter release was inhibited. Neither the slices nor the perfusion-fixed material showed evidence for a separate population of Asp containing axospinous terminals in the areas analyzed. (This does not preclude the existence of such terminals in other brain regions).

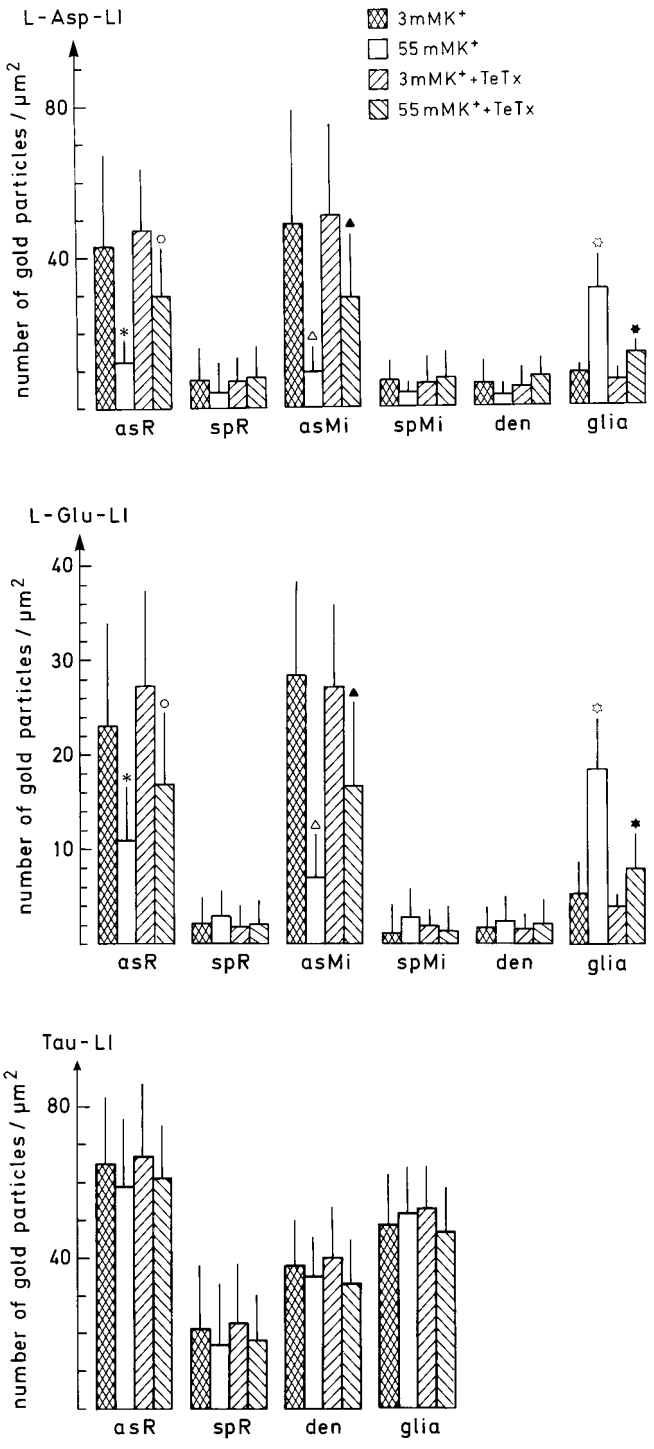

Figure 6. Double-labeling quantitation of amino acids in different tissue compartments in slices preincubated for 2 hr at 3 mM K^+ with or without TeTx (Statens Seruminstitut) before incubation for 1 hr at 3 or 55 mM K^+. The values are mean numbers of gold particles per square micrometer ± SD in *n*-tissue element profiles corrected for background density (particles per square micrometer) over empty resin (average 1.1, 1.6, and 1.8 for the L-Asp, the L-Glu, and the Tau antiserum, respectively). The data shown here are from one animal, similar results were obtained in two other animals in separate experiments. For symbols and other details, see Figure 3. The *top two* panels show *L-Asp-LI* and *L-Glu-LI*, respectively, determined by double labeling on the same ultrathin section (i.e., Asp and Glu were recorded in the same profiles). The *bottom panel* shows *Tau-LI* determined by single labeling. Note that Tau-LI is unaffected by depolarization and TeTX. *Asterisks* and *open triangles*, Values in *asR* and *asMi* at 55 mM K^+ (n = 22 and 19) were significantly different ($p < 0.01$) from the values at 3 mM K^+ with (n = 23 and 20) and without (n = 29 and 21) TeTx and from the values at 55 mM K^+ with TeTx (n = 25 and 19). *Open circles* and *filled triangles*, Values in *asR* and *asMi* at 55 mM K^+ with TeTx were significantly different ($p < 0.01$) from the values at 3 mM K^+ ± TeTx. *Open stars*, Values in glia at 55 mM K^+ (n = 9) were significantly different ($p < 0.01$) from the values at 3 mM K^+ with (n = 8) and without (n = 12) TeTx and from the values at 55 mM K^+ with TeTx (n = 10). *Filled stars*, Values in glia at 55 mM K^+ with TeTx are significantly different ($p < 0.05$) from the values at 3 mM K^+ ± TeTx.

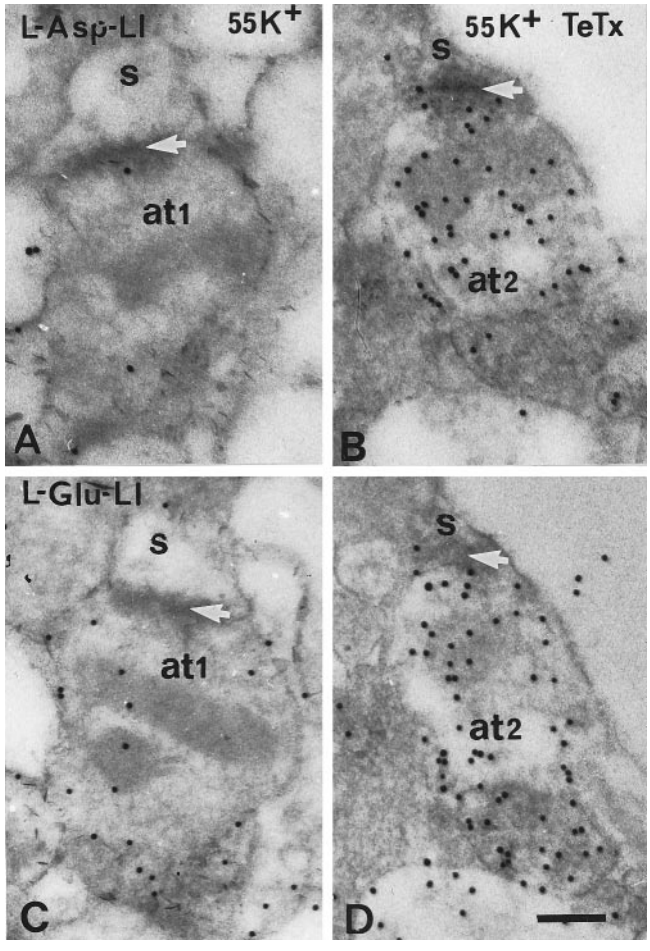

Figure 7. L-Asp-LI (*A*, *B*) and L-Glu-LI (*C*, *D*) in neighboring ultrathin sections showing terminals (*at1* and *at2*) forming synapses with asymmetrical specializations (*white arrows*) on spines (*s*) in stratum radiatum of CA1. The terminal (*at1*) in *A* and *C* was incubated at 55 mM K^+ after preincubation in the absence of TeTx. The terminal (*at2*) in *B* and *D* was incubated at 55 mM K^+ after preincubation in the presence of TeTx. Note that at1 is very weakly labeled with both antisera, whereas at2 is strongly L-Asp- and L-Glu-positive. Note that the spines have low levels of L-Asp and L-Glu immunoreactivities in both experimental conditions. To allow access of TeTx, the terminals sampled here and in Figure 6 are from the superficial 30 μm of the slices. Scale bar, 0.2 μm.

Vesicular localization of aspartate in normoglycemic tissue

To investigate the *in vivo* association of Asp with synaptic vesicles in the intact nonhypoglycemic brain, we used immunogold labeling of perfusion-fixed hippocampi embedded in "antigen-friendly" methacrylate resin (Lowicryl HM20) at low temperature after freeze-substitution (Fig. 12). [This type of material was

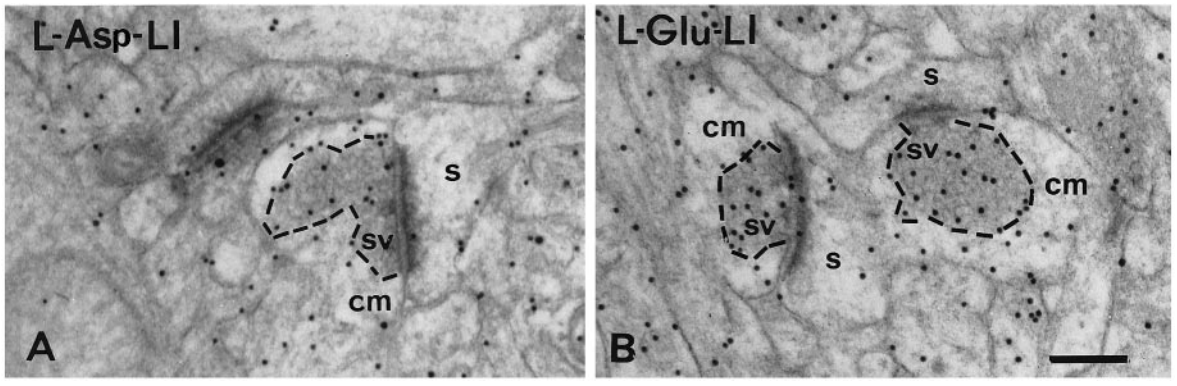

Figure 8. Electron micrographs of L-Asp-LI and L-Glu-LI in hippocampus CA1 from a hypoglycemic rat subjected to perfusion fixation. *A* and *B* show accumulation of immunoreactivities over synaptic vesicle clusters (*sv*) versus over cytoplasmic matrix (*cm*) in terminals making asymmetrical synapses on spines (*s*). *Broken lines* mark the boundary between the vesicle-rich and vesicle-poor parts of the terminals. Scale bar, 0.2 μm.

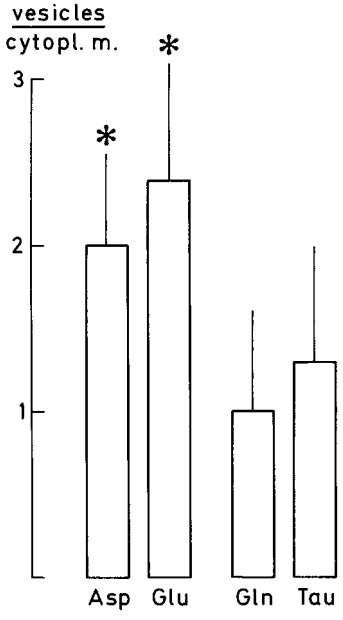

Figure 9. L-Asp (*Asp*), L-Glu (*Glu*), glutamine (*Gln*), and taurine (*Tau*) labeling ratios between vesicle clusters (*vesicles*) and cytoplasmic matrix (*cytopl. m.*) in terminals forming asymmetrical synapses on spines in stratum radiatum CA1 of a rat made hypoglycemic before perfusion fixation (Fig. 8). The ratios were calculated by dividing the densities (particles per square micrometer immunogold particles over the vesicle clusters with the densities over cytoplasmic matrix and are presented as mean ± SD of n profiles) (n = 31, 21, 18, and 20 for Asp-LI, Glu-LI, Gln-LI, and Tau-LI, respectively). *Asterisks*, Ratios produced by the L-Asp and the L-Glu antisera were significantly different ($p < 0.02$) from the ratios produced by the Gln and Tau antisera. The ratios for L-Asp and L-Glu were not significantly different, neither were the ratios for Gln and Tau.

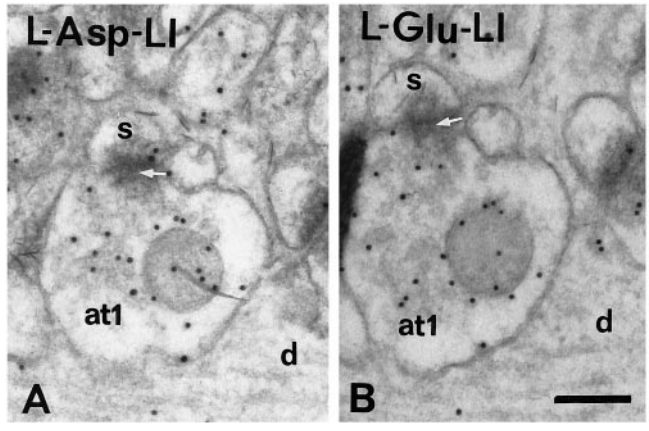

Figure 10. Neighboring ultrathin sections of the same tissue block as in Figure 8 showing colocalization of L-Asp (*A*) and L-Glu (*B*) immunogold particles in a terminal (*at1*) with asymmetrical synaptic specialization (*arrows*) on a spine (*s*). Note that the terminal has high levels of both immunoreactivities, whereas the spines and dendritic shafts (*d*) are very weakly labeled. Scale bar, 0.2 μm.

chosen because pilot experiments in hippocampus showed that it produced higher Asp labeling than tissue embedded in epoxy resin (cf. Usami and Ottersen, 1996, for Asp labeling of Lowicryl-embedded tissue from inner ear)]. The morphology was good enough to determine whether or not a gold particle was overlying the profile of an individual synaptic vesicle (Fig. 12). In excitatory terminals Asp and Glu immunogold particle densities were about three times as high over synaptic vesicles as over cytoplasmic matrix (Fig. 13). This was not the case for Gln immunogold particles, which were evenly distributed between synaptic vesicle profiles and cytoplasmic matrix. [For Glu vs Gln, corresponding results have been found in excitatory spinocerebellar terminals (Ji et al., 1991)].

Because the combined dimensions of antibodies and gold particles are similar to those of synaptic vesicles and to the section thickness, some of the antigenic sites within vesicles will give rise to particles outside the vesicular profiles, and vice versa. To partly overcome these problems, computer analysis of the distance between the center of a gold particle and the center of the nearest synaptic vesicle was performed in Asp- and Gln-labeled terminals. The distributions were significantly different (Fig. 14). Thus, Asp particles were centered over synaptic vesicles (i.e., with their centers within 20 nm from the center of a vesicular profile) twice as frequently as Gln particles, again indicating a clear association of Asp with synaptic vesicles.

DISCUSSION

Asp is released by exocytosis

Our observations suggest that Asp is released by exocytosis together with Glu at hippocampal excitatory synapses: (1) Asp immunogold particles are colocalized with Glu-LI in nerve terminals with morphological features typical of the Schaffer collat-

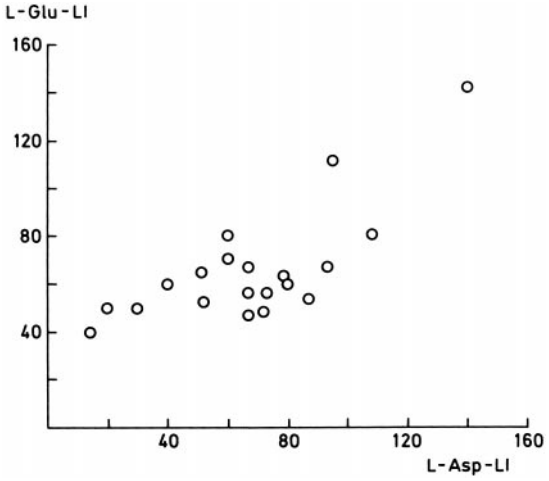

Figure 11. Scatter diagram of the densities of L-Asp-LI and L-Glu-LI in the same nerve endings making asymmetrical junctions with spines in neighboring ultrathin sections from a hypoglycemic rat subjected to perfusion fixation (Fig. 9). The values along the *x*- and *y*-axes are numbers of gold particles per square micromolar. Each *circle* represents the densities of L-Asp-LI and L-Glu-LI over an individual profile, corrected for background labeling over empty resin (1.0 and 1.7 gold particles per square micromolar, respectively). There was a significant positive correlation ($r = 0.73$, $p < 0.01$) between the density of L-Asp-LI and that of L-Glu-LI.

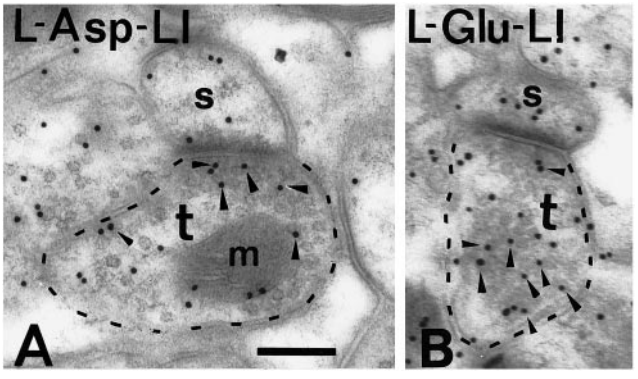

Figure 12. Electron micrograph of normoglycemic perfusion-fixed tissue embedded in Lowicryl by freeze-substitution showing L-Asp-LI (*A*) and L-Glu-LI (*B*) in excitatory-type terminals (*t*) in st. radiatum of CA1. Immunogold particles with their centers inside the outer border of a synaptic vesicle profile, as analyzed in Figure 13, are marked by *arrowheads*. *Broken lines* indicate the outer borders of the terminals. *s*, Dendritic spines; *m*, mitochondrion. Scale bar, 0.2 μm.

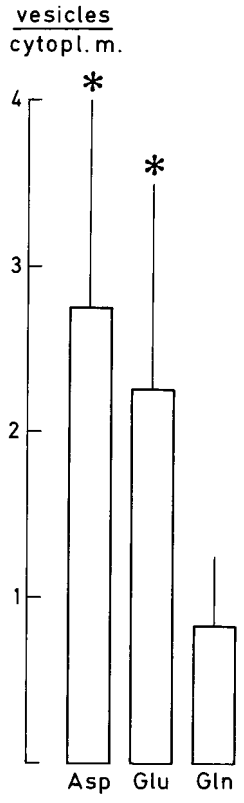

Figure 13. L-Asp-LI and L-Glu-LI, but not Gln-LI are associated with synaptic vesicles in terminals forming asymmetrical synapses on spines in normoglycemic perfusion-fixed hippocampus CA1 st. radiatum. The columns show the ratio of L-Asp ($n = 23$), L-Glu ($n = 12$), and Gln ($n = 12$) labeling densities between synaptic vesicles (*vesicles*) and cytoplasmic matrix (*cytopl. m.*). Unlike in Figure 9, the immunodensities over synaptic vesicles are the number of gold particles with centers within individual synaptic vesicle profiles per total area of synaptic vesicle profile. The ratios were calculated for each terminal by dividing the L-Asp, L-Glu, and Gln densities over synaptic vesicles with the densities over cytoplasmic matrix. *Asterisks*, Similar L-Asp- and L-Glu-labeling ratios, statistically significantly higher than the Gln-labeling ratio ($p < 0.0001$).

eral, commissural, and other excitatory nerve endings (Andersen, 1975; Cotman et al., 1987; Ottersen and Storm-Mathisen, 1989); (2) In these terminals, Asp-LI, similar to Glu-LI but unlike Gln-LI and Tau-LI, is concentrated over the synaptic vesicles relative to the surrounding cytoplasmic matrix; (3) Blocking exocytosis by low Ca^{2+} media or TeTx reduced the depolarization-induced loss of Asp-LI and Glu-LI from excitatory terminals to similar extents, indicating that Asp, like Glu, is released by exocytosis of synaptic vesicles. The fact that low Ca^{2+} and TeTx reduced the accumulation of Asp and Glu in glial cells during depolarization is assumed to reflect reduced uptake of these amino acids subsequent to their attenuated release from the terminals. Unlike Asp-LI and Glu-LI, Tau-LI was unaffected by depolarization and TeTx. This supports the idea that changes in Asp-LI and Glu-LI reflect changes in synaptic release. The Tau results further add to the notion that Tau does not act as a transmitter at synapses in the CNS (Shupliakov et al., 1994).

Our data strongly suggest that the Asp depletion observed here is at least partly attributable to exocytotic release. Particularly compelling is our finding that Asp is as closely associated with synaptic vesicles as is Glu, the established transmitter in the major excitatory hippocampal pathways (Bramham et al., 1990). This does not necessarily imply that exocytosis is alone responsible for the loss of Asp observed in our study. Nonexocytotic release, probably mediated by reverse operation of glutamate–aspartate transporters, which are situated on excitatory nerve terminals in the hippocampus (Gundersen et al., 1993), is likely to contribute, as judged by our observation that TeTx or low Ca^{2+} did not fully prevent the K^+-induced depletion of Asp and Glu. In the case of TeTx these observations are compatible with a study in synaptosomes showing that Glu release was inhibited by ~70%, whereas Asp release was almost totally inhibited (McMahon et al., 1992).

One must also consider the possibility that exchange of Asp with synaptically released Glu may contribute to the Asp depletion. Such heteroexchange would occur through plasma membrane glutamate transporters, which are known to transport both

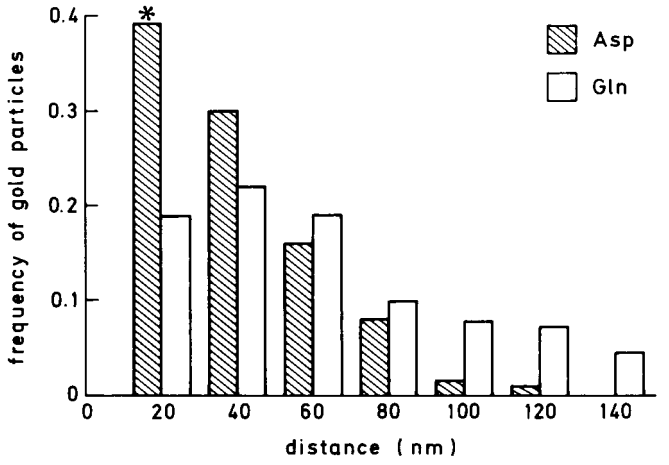

Figure 14. L-Asp immunogold particles are more frequently located close to vesicle profiles than Gln immunogold particles. The distances of the centers of gold particles from the centers of synaptic vesicles were sorted into bins of 20 nm. The *columns* show the frequencies of inter-center distances for each 20 nm bin. The total numbers of Asp and Gln immunogold particles were 139 and 271, respectively. Distances >140 nm (data not shown) make up altogether 4 and 7% for L-Asp and Gln immunogold particles, respectively. *Asterisk*, Within a distance of 20 nm from the center of the vesicle profile, the frequency of L-Asp immunogold particles is significantly higher than that of Gln immunogold particles ($p < 0.0001$, see Materials and Methods).

Asp and Glu with similar affinities (Balcar and Johnston, 1972; Arriza et al., 1994; Danbolt, 1994). The importance of this mechanism depends on the size of the cytosolic pool of Asp that is accessible to the excitatory amino acid transporters. Our finding that Asp is preferentially associated with the synaptic vesicle clusters suggests that heteroexchange plays a minor role in the terminals under these conditions. It is of relevance that Zhou et al. (1995), based on experiments on isolated nerve terminals from CA1, concluded that the K^+-evoked release of Asp is not secondary to reuptake of synaptically released Glu that was removed by fast superfusion.

It remains to discuss the possibility that Asp is depleted secondary to a transamination to Glu through the action of Asp-AT. If this were the sole mechanism responsible for Asp depletion, the implication would be that Asp simply serves as a reservoir for synaptically releasable Glu. This is not likely to be the case. A major contribution of this mechanism would be contrary to our finding that inhibition of Asp-AT with AOAA had no effect on the Asp and Glu staining in depolarized or control slices (see also Storm-Mathisen et al., 1986) and is not compatible with the wealth of data showing that a release of Asp to the extracellular space does occur Ca^{2+} dependently on membrane depolarization (Nadler et al., 1976; Toggenburger et al., 1983; Fonnum et al., 1986; Girault et al., 1986; Paulsen and Fonnum, 1989; Kangrga and Radic, 1990; Roisin et al., 1991; Klancnick et al., 1992; Fleck et al., 1993; Zhou et al., 1995).

In conclusion, the present data suggest that excitatory nerve terminals in the hippocampus are capable of coreleasing Asp and Glu by an exocytotic mechanism. Our findings imply that Asp and Glu may act as bona fide cotransmitters in certain fiber systems. It should be noted that the fiber pathways studied here are presynaptic to glutamate receptors (NMDA receptors) that show affinities for both amino acids and are exposed to both Asp and Glu released Ca^{2+} dependently, the Asp effect being augmented by low glucose (Fleck et al., 1993).

Are the slice results valid for the *in vivo* situation?

One must be cautious to extrapolate from slices to the *in vivo* situation. Although the present slice data suggest that excitatory nerve terminals are endowed with the capacity for corelease of Asp and Glu, they cannot be used to predict the relative contribution of the two amino acids to the total releasable pool *in vivo*. In fact it is our general experience that the immunogold signal for Asp in nerve terminals is considerably stronger in slices than in sections of perfusion-fixed brains (see below), which should be more representative of the *in vivo* situation. The explanation for this discrepancy is unknown. It could reflect a demasking of Asp caused by *in vitro* incubation, but is more likely an effect of the slightly perturbed energy status that may prevail even in slices that are optimally supplied with oxygen and energy substrates (cf. Whittingham, 1986). This would be consistent with the data showing that hypoglycemia is associated with an increased content (present data) and release (Fonnum et al., 1986; Sandberg et al., 1986; Nadler et al., 1990) of Asp from excitatory fiber systems. Biochemical mechanisms have been offered to explain the shift in Glu—Asp ratio that occurs during hypoglycemia (Fonnum, 1988). In this study we have taken advantage both of this shift and of freeze-substituted normal tissue as means of enhancing the Asp signal to an extent that permits a quantitative analysis of the subcellular antigen distribution. The results show that the hypoglycemia-induced increment in Asp comprises a synaptic vesicular pool, and that vesicular Asp localization is also present in the normal hippocampus.

What is the metabolic source for formation of nerve terminal Asp?

When excitatory type of terminals were depolarized in the presence of Gln at normal extracellular concentration, the contents of Asp and Glu were sustained (see also Gundersen et al., 1991). This shows that Gln can act as a precursor not only for Glu, but also for exocytotically releasable Asp. When exposing the slices to intermediate depolarizing conditions with Gln (40 mM K^+), the level of Asp increased (by 23% compared with 5 mM K^+ with Gln) in this category of terminal. This indicates that excitatory terminals may increase their synthesis of Asp to keep pace with an increased rate of Asp release during high synaptic activity. Stimulation has been observed to be associated with a shift toward relatively more Asp than Glu being released and contained in hippocampal slices (Szerb, 1988).

The transmitter status of aspartate

The increased insight gained by recent studies (cf. Fleck et al., 1993; Zhou et al., 1995), including the present one, has strengthened the evidence for a transmitter role of Asp in excitatory fiber systems in the hippocampus. Our results show that a transmitter pool of Asp may be disclosed under experimental conditions that elevate the Asp contents of the nerve terminals or in nonhypoglycemic tissue prepared to obtain high immunocytochemical sensitivity. It remains to be seen whether this conclusion holds for most or only a limited proportion of the major excitatory pathways in the brain and to what extent the pathways vary the released Asp–Glu ratio in different conditions.

Another impediment to a general acceptance of Asp as transmitter has been the apparent lack of vesicular uptake. The clear association between Asp and synaptic vesicles in "intact" tissue (present observations) suggests that the lack of demonstrable Asp uptake in reduced systems (Naito and Ueda, 1983; Maycox et al., 1988; Burger et al., 1991; Fykse et al., 1992) might be related to

methodology. In line with this view are the recent reports that endogenous Asp is localized in and released by exocytosis from microvesicles in glutamatergic neuroendocrine pinealocytes (Yatsushiro et al., 1997) and that exogenous D-[^{3}H]Asp enters synaptic vesicles and is released by exocytosis from cultured cerebellar granule cells (Cousin et al., 1997; Cousin and Nicholls, 1997). Nonetheless, our previous failure to detect significant enrichment of endogenous L-Asp or exogenous D-Asp at synapses formed by lamprey reticulospinal and dorsal column axons (Gundersen et al., 1995) suggests that the present findings may not be valid for all excitatory systems or all species.

An important outstanding issue pertains to the quantitative significance of Asp versus Glu as an excitatory transmitter. It also remains to be resolved whether Asp may serve signal roles in addition to that as a classical transmitter.

REFERENCES

Amiry-Moghaddham M, Nagelhus E, Ottersen OP (1994) Light and electron microscopic distribution of taurine, an organic osmolyte, in rat renal tubule cells. Kidney Int 45:10–22.

Andersen P (1975) Organization of hippocampal neurons and their interconnections. In: The hippocampus (Isaacson RL, Pribram KH, eds), pp 155–175. New York: Plenum.

Arriza JL, Fairman WA, Wadiche JI, Murdoch GH, Kavanaugh MP, Amara SG (1994) Functional comparison of three glutamate transporter subtypes cloned from human motor cortex. J Neurosci 14:5559–5569.

Balcar V, Johnston GAR (1972) The structural specificity of the high affinity uptake of L-glutamate and L-aspartate by rat brain slices. J Neurochem 19:2657–2666.

Bramham CR, Torp R, Zhang N, Storm-Mathisen J, Ottersen OP (1990) Distribution of glutamate-like immunoreactivity in excitatory hippocampal pathways: a semiquantitative electron microscopic study in rats. Neuroscience 39:405–417.

Broman J, Anderson S, Ottersen OP (1993) Enrichment of glutamate-like immunoreactivity in primary afferent terminals throughout the spinal cord dorsal horn. Eur J Neurosci 5:1050–1061.

Burger PM, Hell J, Mehl E, Baumert M, Krasel C, Lottspeich F, Jahn R (1991) GABA and glycine in synaptic vesicles: storage and transport characteristics. Neuron 7:287–293.

Chaudhry FA, Lehre KP, Van Lookeren Campagne M, Ottersen OP, Danbolt NC, Storm-Mathisen J (1995) Glutamate transporters in glial plasma membranes: highly differentiated localizations revealed by quantitative ultrastructural immunocytochemistry. Neuron 14:711–720.

Cotman CW, Monaghan DT, Ottersen OP, Storm-Mathisen J (1987) Anatomical organization of excitatory amino acid receptors and their pathways. Trends Neurosci 10:273–280.

Cousin MA, Nicholls DG (1997) Synaptic vesicle recycling in cultured cerebellar granule cells: role of vesicular acidification and refilling. J Neurochem 69:1927–1935.

Cousin MA, Hurst H, Nicholls DG (1997) Presynaptic calcium channels and field-evoked transmitter exocytosis from cultured cerebellar granule cells Neuroscience 81:151–161.

Danbolt NC (1994) The high affinity uptake system for excitatory amino acids in the brain. Prog Neurobiol 44:377–396.

Dunlop DS, Neidle A, McHale D, Dunlop DM, Lajtha A (1986) The presence of free D-aspartic acid in rodents and man. Biochem Biophys Res Commun 141:27–32.

Engelsen B, Fonnum F (1983) Effects of hypoglycemia in the transmitter pool and the metabolic pool of glutamate in rat brain. Neurosci Lett 42:317–322.

Ericson AC, Blomqvist A, Craig AD, Ottersen OP, Broman J (1995) Evidence for glutamate as neurotransmitter in trigemino- and spinothalamic tract terminals in the nucleus submedius of cats. Eur J Neurosci 7:305–317.

Fleck MW, Henze DA, Barrionuevo G, Palmer AM (1993) Aspartate and glutamate mediate excitatory synaptic transmission in area CA1 of the hippocampus. J Neurosci 13:3944–3955.

Fonnum F (1984) Glutamate: a neurotransmitter in mammalian brain. J Neurochem 42:1–11.

Fonnum F (1988) Excitatory amino acid pathways and the biochemical architecture of the glutamate terminal. In: Frontiers in excitatory amino acid research (Cavalihero E, Lehmann J, Turski L, eds), pp 85–92. New York: Liss.

Fonnum F, Paulsen RH, Fosse VM, Engelsen B (1986) Synthesis and release of amino acid transmitters. Adv Exp Med Biol 203:285–293.

Fykse EM, Fonnum F (1988) Uptake of gamma-aminobutyric acid by a synaptic vesicle fraction isolated from rat brain. J Neurochem 50:1237–1242.

Fykse EM, Iversen EG, Fonnum F (1992) Inhibition of L-glutamate uptake into synaptic vesicles. Neurosci Lett 135:125–128.

Girault JA, Barbeito L, Spampinato U, Gozlan H, Glowinski J, Besson M-J (1986) *In vivo* release of endogenous amino acids from the rat striatum: further evidence for a role of glutamate and aspartate in corticostriatal neurotransmission. J Neurochem 47:98–106.

Gundersen HJ, Bendtsen TF, Korbo L, Marcussen N, Møller A, Nielsen K, Nyengaard JR, Pakkenberg B, Sørensen FB, Vesterby A (1988) Some new, simple and efficient stereological methods and their use in pathological research and diagnosis. APMIS 96:379–394.

Gundersen V, Ottersen OP, Storm-Mathisen J (1991) Aspartate- and glutamate-like immunoreactivities in rat hippocampal slices: depolarization-induced redistribution and effects of precursors. Eur J Neurosci 3:1281–1299.

Gundersen V, Danbolt NC, Ottersen OP, Storm-Mathisen J (1993) Demonstration of glutamate/aspartate uptake activity in nerve endings by use of antibodies recognizing exogenous D-aspartate. Neuroscience 57:97–111.

Gundersen V, Shupliakov O, Brodin L, Ottersen OP, Storm-Mathisen J (1995) Quantification of excitatory amino acid uptake at intact glutamatergic synapses by immunocytochemistry of exogenous D-aspartate. J Neurosci 15:4417–4428.

Harris KM, Sultan P (1995) Variation in the number, location and size of synaptic vesicles provides an anatomical basis for the nonuniform probability of release at hippocampal CA1 synapses. Neuropharmacology 34:1387–1395.

Hashimoto A, Nishikawa T, Oka T, Hayashi T, Takahashi K (1993) Widespread distribution of free D-aspartate in rat periphery. FEBS Lett 331:4–8.

Headley PM, Grillner S (1990) Excitatory amino acids and synaptic transmission: the evidence for a physiological function. Trends Pharmacol Sci 11:205–211.

Hsu SM, Raine L, Fanger H (1981) Use of avidin-biotin-peroxidase complex (ABC) in immunoperoxidase techniques: a comparison between ABC and unlabeled antibody (PAP) procedures. J Histochem Cytochem 29:577–580.

Ji Z, Aas JE, Laake J, Walberg F, Ottersen OP (1991) An electron microscopic analysis of glutamate and glutamine in terminals of rat spinocerebellar fibers. J Comp Neurol 307:296–310.

Kangrga I, Randic M (1990) Tachykinins and calcitonin gene-related peptide enhance release of endogenous glutamate and aspartate from the rat spinal dorsal horn slice. J Neurosci 10:2026–2038.

Klancnik JM, Cuénod M, Gahwiler BH, Jiang ZP, Do K (1992) Release of endogenous amino acids, including homocysteic acid and cysteine sulphinic acid, from rat hippocampal slices evoked by electrical stimulation of Schaffer collateral-commisural fibres. Neuroscience 49:557–570.

Kvamme E (1983) Glutaminase (PAG). Neurol Neurobiol 7:51–67.

Laake JH, Gundersen V, Nordbø G, Ottersen OP, Storm-Mathisen J (1986) An antiserum against glutamine. In: Excitatory amino acids (Roberts PJ, Storm-Mathisen J, Bradford HF, eds), pp 448–450. London: Macmillan.

Link E, Edelmann L, Chou JH, Binz T, Yamasaki S, Eisel U, Baumert M, Sudhof TC, Niemann H, Jahn R (1992) Tetanus toxin action: inhibition of neurotransmitter release linked to synaptobrevin proteolysis. Biochem Biophys Res Comm 189:1017–1023.

Link E, Blasi J, Chapman ER, Edelmann L, Baumeister A, Binz T, Yamasaki S, Niemann H, Jahn R (1994) Tetanus and botulinum neurotoxins. Tools to understand exocytosis in neurons. In: Molecular and cellular mechanisms of neurotransmitter release (Stjärne L, Greengard P, Grillner S, Hökfelt T, Ottoson D, eds), pp 47–58. New York: Raven.

Leergaard TB, Bjaalie JG (1995) Semi-automatic data acquisition for quantitative neuroanatomy. Micro Trace: computer program for recording of spatial distribution of neuronal populations. Neurosci Res 22:231–243.

Maxwell DJ, Christie WM, Short AD, Storm-Mathisen J, Ottersen OP (1990) Central boutons of glomeruli in the spinal cord of the cat are

enriched with L-glutamate-like immunoreactivity. Neuroscience 36:83–104.
Maycox PR, Deckwerth T, Hell JW, Jahn R (1988) Glutamate uptake by brain synaptic vesicles. J Biol Chem 263:15423–15428.
McMahon HT, Foran P, Dolly JO, Verhage M, Wiegant VM, Nicholls DG (1992) Tetanus toxin and botulinum toxins type A and B inhibit glutamate, gamma-aminobutyric acid, aspartate, and met-enkephalin release from synaptosomes: clues to the locus of action. J Biol Chem 267:21338–21343.
Merighi A, Polak JM, Theodosis DT (1991) Ultrastructural visualization of glutamate and aspartate immunoreactivities in the rat dorsal horn, with special reference to the co-localization of glutamate, substance P and calcitonin-gene related peptide. Neuroscience 40:67–80.
Montero VM (1994) Quantitative immunogold evidence for enrichment of glutamate but not aspartate in synaptic terminals of retinogeniculate, geniculo-cortical, and cortico-geniculate axons in the cat. Vis Neurosci 11:675–681.
Nadler JV, Vaca KW, White WF, Lynch GS, Cotman CW (1976) Aspartate and glutamate as possible transmitter of excitatory hippocampal afferents. Nature 260:538–540.
Nadler JV, Martin D, Bustos GA, Burke SP, Bowe MA (1990) Regulation of glutamate and aspartate release from the Schaffer collaterals and other projections of CA3 hippocampal pyramidal cells. Prog Brain Res 83:115–130.
Naito S, Ueda T (1983) ATP-dependent uptake of glutamate into protein I-associated synaptic vesicles. J Biol Chem 258:696–699.
Nicholls DG (1989) Release of glutamate, aspartate, and γ-aminobutyric acid from isolated nerve terminals. J Neurochem 52:331–341.
Nicholls DG (1993) The glutamatergic nerve terminal. Eur J Biochem 212:613–631.
Ottersen OP (1987) Postembedding light-and electron microscopic immunocytochemistry of amino acids: description of a new model system allowing identical conditions for specificity testing and tissue processing. Exp Brain Res 69:167–174.
Ottersen OP (1989a) Quantitative electron microscopic immunocytochemistry of amino acids. Anat Embryol 180:1–15.
Ottersen OP (1989b) Postembedding immunogold labeling of fixed glutamate: an electron microscopic analysis of the relationship between gold particle density and antigen concentration. J Chem Neuronanat 2:57–67.
Ottersen OP, Storm-Mathisen J (1984a) Neurons containing or accumulating transmitter amino acids. In: Handbook of chemical neuroanatomy, Vol 3 (Björklund A, Hökfelt T, Kuhar MJ, eds), pp 141–246. Amsterdam: Elsevier.
Ottersen OP, Storm-Mathisen J (1984b) Glutamate-and GABA-containing neurons in the mouse and rat brain as demonstrated with a new immunocytochemical technique. J Comp Neurol 229:374–392.
Ottersen OP, Storm-Mathisen J (1989) Excitatory and inhibitory amino acids in the hippocampus. Neurol Neurobiol 52:97–117.
Ottersen OP, Zhang N, Walberg F (1992) Metabolic compartmentation of glutamate and glutamine: morphological evidence obtained by quantitative immunocytochemistry in rat cerebellum. Neuroscience 46:519–534.
Paulsen RE, Fonnum F (1989) Role of glial cells for the basal and Ca^{2+}-dependent K^{+}-evoked release of transmitter amino acids investigated by microdialysis. J Neurochem 52:1823–1829.
Phend KD, Weinberg RJ, and Rustioni A (1992) Techniques to optimize post-embedding single and double staining for amino acid neurotransmitters. J Histochem Cytochem 40:1011–1020.
Roisin MP, Brassart JL, Charton G, Crepel V, Ben Ari Y (1991) A new method for the measurement of endogenous transmitter release in localized regions of hippocampal slices. J Neurosci Methods 37:183–189.
Sandberg M, Butcher SP, Hagberg H (1986) Extracellular overflow of neuroactive amino acids during severe insulin-induced hypoglycemia: *in vivo* dialysis of the rat hippocampus. J Neurochem 47:178–184.
Schiavo G, Benfenati F, Poulain B, Rosetto O, Polverino de Laureto P, DasGupta B, Montecucco C (1992) Tetanus and botulinum-B neurotoxins block neurotransmitter release by proteolytic cleavage of synaptobrevin. Nature 359:832–835.
Shupliakov O, Brodin L, Srinivasan M, Grillner S, Cullheim S, Storm-Mathisen J, Ottersen OP (1994) Extrasynaptic localization of taurine-like immunoreactivity in the lamprey spinal cord. J Comp Neurol 347:301–311.
Somogyi P, Halasy K, Somogyi J, Storm-Mathisen J, Ottersen OP (1986) Quantification of immunogold labeling reveals enrichment of glutamate in mossy and parallel fibre terminals in cat cerebellum. Neuroscience 19:1045–1050.
Storm-Mathisen J, Leknes AK, Bore A, Vaaland JL, Edminson P, Haug FMS, Ottersen OP (1983) First visualization of glutamate and GABA in neurones by immunocytochemistry. Nature 301:517–520.
Storm-Mathisen J, Ottersen OP, Fu-Long T, Gundersen V, Laake JH, Nordbø G (1986) Metabolism and transport of amino acids studied by immunocytochemistry. Med Biol 64:127–132.
Szerb JC (1988) Changes in the relative amounts of aspartate and glutamate released and retained in hippocampal slices during stimulation. J Neurochem 50:219–224.
Toggenburger G, Wiklund L, Henke H, Cuénod M (1983) Release of endogenous and accumulated exogenous amino acids from slices of normal and climbing fibre-deprived rat cerebellar slices. J Neurochem 41:1606–1613.
Tracey DJ, Biasi SDe, Phend K, Rustioni A (1991) Aspartate-like immunoreactivity in primary afferent neurons. Neuroscience 40:673–686.
Usami S, Ottersen OP (1996) Aspartate is enriched in sensory cells and subpopulations of non-neuronal cells in the guinea pig inner ear: a quantitative immunoelectron microscopic analysis. Brain Res 742:43–49.
Van den Pol AN (1991) Glutamate and aspartate immunoreactivity in hypothalamic presynaptic axons. J Neurosci 11:2087–2101.
Wang BL, Larsson LI (1985) Simultaneous demonstration of multiple antigens by indirect immunofluorescence or immunogold staining: novel light and electron microscopical double and triple staining method employing primary antibodies from the same species. Histochemistry 83:47–56.
Whittaker VP, Michaelson IA, Kirkland RJ (1964) The separation of synaptic vesicles from nerve-ending particles (synaptosomes). Biochem J, 90:293–303.
Whittingham TS (1986) Metabolic studies in the hippocampal slice preparation. In: Brain slices: fundamentals, applications and implications (Schurr A, Teyler TJ, Tseng MT, eds), pp 59–69. Basel: Karger.
Yatsushiro S, Yamada H, Kozaki S, Kumon H, Michibata H, Yamamoto A, Moriyama Y (1997) L-aspartate but not the D form is secreted through microvesicle-mediated exocytosis and is sequestred through Na^{+}-dependent transporter in rat pinealocytes. J Neurochem 69:340–347.
Zhang N, Walberg F, Laake JH, Meldrum BS, Ottersen OP (1990) Aspartate-like and glutamate-like immunoreactivities in the inferior olive and climbing fibre system: a light microscopic and semiquantitative electron microscopic study in rat and baboon (papio anubis). Neuroscience 38:61–80.
Zhang N, Storm-Mathisen J, Ottersen OP (1993) A model system for specificity testing and antigen quantitation in single and double labeling postembedding electron microscopic immunocytochemistry. Neurosci Protocols 13:1–20.
Zhou M, Peterson CL, Lu YB, Nadler V (1995) Release of glutamate and aspartate from CA1 synaptosomes: selective modulation of aspartate release by ionotropic glutamate receptor ligands. J Neurochem 64:1556–1566.